Journal of Magnetic Resonance 209 (2011) 347–351

Contents lists available at ScienceDirect

Journal of Magnetic Resonance

journal homepage: www.elsevier.com/locate/jmr

Communication

Inhomogeneity-free heteronuclear iMQC

Rosa T. Branca *, Elizabeth R. Jenista, Warren S. Warren

Department of Chemistry, Duke University, Durham, NC 27708, United States

ARTICLE INFO

Article history:
Received 2 August 2010
Revised 29 December 2010
Available online 22 January 2011

Keywords:
Intermolecular multiple quantum coherence
CRAZED sequence
^{13}C hyperpolarization
Dynamic nuclear polarization

ABSTRACT

Intermolecular dipolar interactions between proton and carbon spins can be used to indirectly detect carbon spectra with high sensitivity. In this communication, we present a modified sequence that, in addition to the high sensitivity of heteronuclear intermolecular multiple quantum coherence (iMQC) experiments, retains the line narrowing capability characteristic of homonuclear zero-quantum coherences. We demonstrate that this sequence can be used to obtain high resolution ^{13}C spectra in the presence of magnetic field inhomogeneities, both for thermal and hyperpolarized samples, and discuss applications to water-hyperpolarized carbon imaging.

1. Introduction

Intermolecular multiple quantum coherences (iMQCs) have been used for the past 20 years to obtain high resolution spectra in the presence of magnetic field inhomogeneities [1–4], and to enhance contrast in MR imaging experiments [5,6]. Coherences between all spins are excited at the same time as the standard NMR signal. In the standard NMR framework, these coherences are typically ignored, since they do not give rise to any observable signal. However, in CRAZED-like experiments (Fig. 1a), where the longitudinal magnetization is modulated to produce an effective non-zero dipolar field, these coherences give rise to a signal which is typically 10–50% of the standard NMR signal and therefore cannot be ignored [7]. Among all coherences, intermolecular zero-quantum coherences (iZQCs) are intrinsically insensitive to inhomogeneous broadening, but combinations of other types of iMQCs can be made to have this same insensitivity [8–10].

One intriguing potential application of iMQCs is in improving imaging with hyperpolarized reagents, specifically hyperpolarized carbon. Many different research groups have been examining potential uses of such hyperpolarized molecules both *in vivo* and *in vitro* [11–14]. The DNP methodology, in particular, is very versatile, and hundreds of different molecules have been polarized. One limitation of virtually all *in vivo* work has been "incoherent imaging" (localized magnetic resonance spectroscopy after one pulse), which is dominated by T_2^* effects. For example, pyruvate and lactate in the TRAMP mouse prostate cancer model were reported as having a 25 Hz linewidth [15]. Recent work with smaller voxels shows that proton decoupling narrows lactate linewidths slightly *in vivo* (10.9 Hz verses 11.8 Hz) [16], but the pixel-to-pixel standard deviation of the lactate and pyruvate linewidths (4.9 Hz and 5.8 Hz respectively) clearly reflect a strong inhomogeneous component.

Can the intrinsic iZQC compensation of inhomogeneous broadening be used to overcome this problem? Without hyperpolarization, low γ nuclei give very weak iMQC signals. The initial growth rate of iDQCs or iZQCs is proportional to γM_o^2, and M_o itself is proportional to γ^2, leading to a net γ^5 dependence of the signal strength. In fact, the first carbon–carbon iMQCs have only recently been reported by groups using hyperpolarization [17]. Heteronuclear iMQCs are a different story. The scaling relationship is much more favorable, and reference [9] shows that heteronuclear zero and double quantum coherences between ^{1}H and ^{13}C can be observed. For these experiments, the CRAZED sequence is slightly modified to take into account the difference in the gyromagnetic ratio between ^{1}H and ^{13}C (for example, since a ^{1}H–^{13}C iZQC evolves at 3/4 the proton resonance frequency, it would be refocused by a 4:3 gradient ratio if ultimately detected as proton magnetization). Unfortunately, for this same reason, heteronuclear ^{13}C–^{1}H iZQCs lead to resonance frequency lines that are only 25% narrower than those obtainable with ^{1}H, but three times broader than those obtainable in ^{13}C homonuclear iZQC experiments.

In order to narrow the resonance frequency lines in the heteronuclear iZQC experiment without incurring in sensitivity loss, we apply a modified version of the CRAZED sequence that accommodates *ad hoc* both double and zero quantum evolutions. This sequence, shown in Fig. 1b, resembles the heteronuclear iDQC (sequence in Fig. 1a with $G_2/G_1 = 5/4$), with the exception of the addition of two selective inversion pulses during the iDQC evolution. These pulses are used to invert the proton magnetization in

* Corresponding author at: 124, Science Drive, 2213 FFSC, Box 90347, Durham, NC 27708, United States.
E-mail address: tamara.branca@duke.edu (R.T. Branca).

1090-7807/$ - see front matter © 2011 Elsevier Inc. All rights reserved.
doi:10.1016/j.jmr.2011.01.018

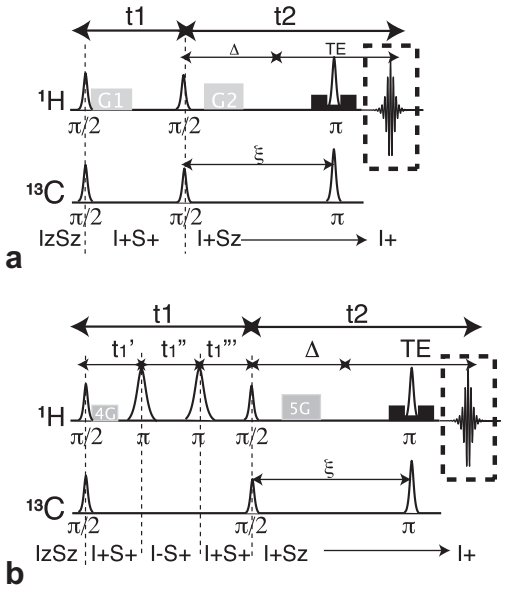

Fig. 1. (a) CRAZED sequence used to detect the signal from intermolecular multiple quantum coherences. The ratio of the area between the second and the first pulsed field gradient designates the selected coherence. For ^{13}C–^{1}H iDQCs, the ratio G_2/G_1 must be set to ±5/4, while for ^{13}C–^{1}H iZQCs, it needs to be set to ±3/4. (b) Modified CRAZED sequence for the detection of inhomogeneity-free heteronuclear iMQCs. The sequence allows evolution of both iDQC and iZQC coherences during the first evolution time $t_1 = t' + t'' + t'''$. During t_1, the iDQCs are transformed into iZQCs by a selective inversion of the ^{1}H spins. A second selective inversion pulse on the ^{1}H spins transforms iZQCs back into iDQCs. A mixing pulse on both the ^{13}C and ^{1}H spins transform the iDQCs into iSQCs, which is then refocused as ^{1}H signal by the long-range dipolar field created by the modulated ^{13}C longitudinal magnetization.

order to transform iDQC (I + S+) coherences into iZQC coherences (I − S+). With this transformation, this sequence can be made inhomogeneity free for the X–^{1}H correlations if the iDQC evolution is carefully compensated by the iZQC evolution. This compensation can be achieved by keeping the t''' delay constant ($\Delta t''' = 0$) and stepping the t' and t'' delays so that:

$$(\gamma_X + \gamma_H)\Delta t_1' + (\gamma_X - \gamma_H)\Delta t_1'' = 0,$$

which means by using a

$$\Delta t_1'' = \frac{(\gamma_X + \gamma_H)}{(\gamma_H - \gamma_X)}\Delta t', \tag{1}$$

with $\frac{1}{SW_{F1}} = \Delta t_1 = \Delta t_1' + \Delta t_1''$.

When this is accomplished, the apparent resonance frequency for the X–^{1}H correlation will be given by

$$\frac{(\Omega_X+\Omega_H)\Delta t_1' + (\Omega_X-\Omega_H)\Delta t_1''}{\Delta t' + \Delta t_1''} = \frac{(\Omega_X+\Omega_H)\Delta t_1' + (\Omega_X-\Omega_H)\frac{(\gamma_X+\gamma_H)}{(\gamma_H-\gamma_X)}\Delta t_1'}{\Delta t' + \frac{(\gamma_X+\gamma_H)}{(\gamma_H-\gamma_X)}\Delta t'} = \\ = \frac{(\Omega_X+\Omega_H)(\gamma_H-\gamma_X)\Delta t_1' + (\Omega_X-\Omega_H)(\gamma_X+\gamma_H)\Delta t_1'}{(\gamma_H-\gamma_X)\Delta t' + (\gamma_X+\gamma_H)\Delta t'} = \Omega_X - \frac{\gamma_X}{\gamma_H}\Omega_H \tag{2}$$

while the echo will be refocused at a time

$$\Delta = \frac{\gamma_X + \gamma_H}{\gamma_H}(t_1' + t_1''') + \frac{\gamma_X - \gamma_H}{\gamma_H}t_1'', \tag{3}$$

after the mixing pulse.

If the X nucleus is a ^{13}C nucleus, since the frequency of the ^{13}C–^{1}H iDQC is −5/3 higher than that of the ^{13}C–^{1}H iZQC, the t_1' and t_1'' delays need to be stepped so that

$$\Delta t_1'' = \frac{5}{3}\Delta t_1'. \tag{4}$$

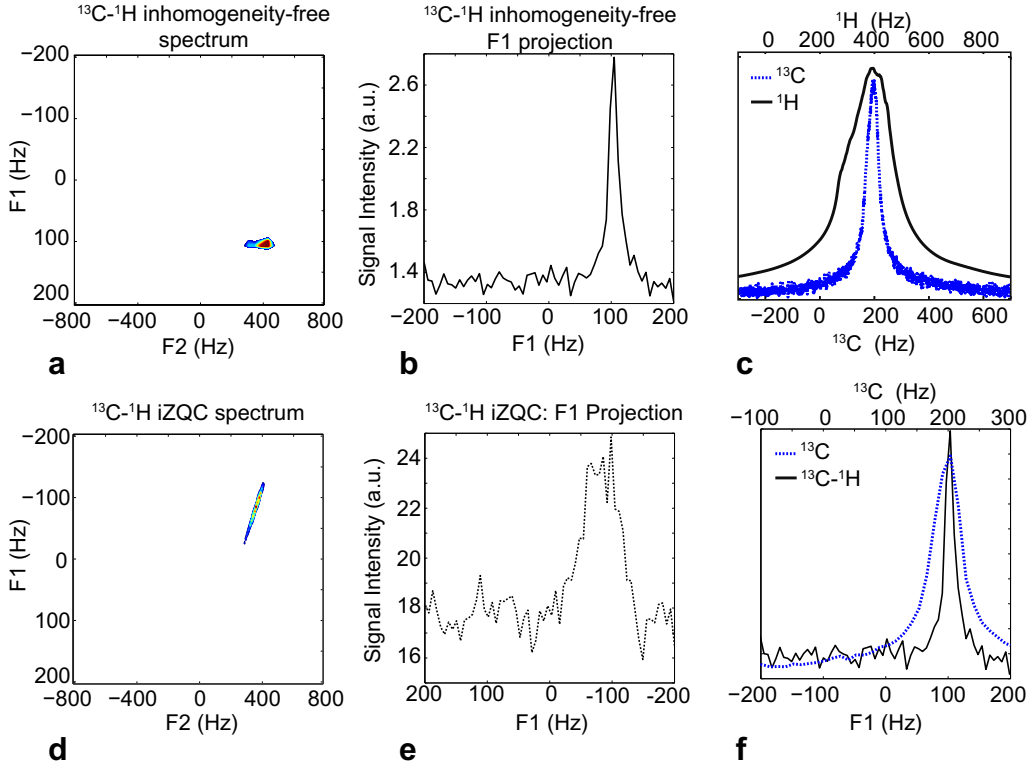

Fig. 2. Experimental demonstration of inhomogeneity-free heteronuclear ^{13}C–^{1}H iMQCs on the urea de-shimmed sample. (a) Spectrum acquired with the sequence in Fig. 1b (b) Projection along the indirectly detected dimension F1. (c) Standard 1D ^{13}C and ^{1}H spectrum of the urea de-shimmed sample. (d) 2D ^{13}C–^{1}H iZQC spectrum acquired with the pulse sequence in Fig. 1a with $G_2/G_1 = -3/4$. (e) Projection of (d) along the indirectly detected dimension F1. (f) Comparison between the standard 1D ^{13}C spectrum and the inhomogeneity-free ^{13}C–^{1}H iMQC spectrum.

The apparent evolution frequency will then be:

$$\frac{(\Omega_C+\Omega_H)3\Delta t_1'+(\Omega_C-\Omega_H)5\Delta t_1'}{3\Delta t'+5\Delta t'}=\Omega_C-\frac{\Omega_H}{4}, \quad (5)$$

and the signal will be refocused at a time

$$\Delta=\frac{5}{4}(t_1'+t_1''')-\frac{3}{4}t_1'', \quad (6)$$

after the mixing pulse.

This means that, in the presence of one proton species, the indirectly detected spectrum will be equivalent to the ^{13}C spectrum, shifted by $-1/4$ of the proton resonance frequency offset Ω_H. In other words, the carbon resonance frequency offset, as well as its inhomogeneous resonance frequency spreading is renormalized by the proton resonance frequency offset rescaled by the gyromagnetic ratio between the carbon and proton nuclei.

2. Results and discussion

For all experiments we use a 7T small animal magnetic resonance tomograph with a 210 mm inner bore diameter, interfaced to a Bruker Biospec console (Bruker BioSpin MRI GmbH, Ettlingen, Germany). The system is equipped with a gradient coil system (maximum gradient strength 42Gauss/cm) and a dual $^1H/^{13}C$ transmitter-receive coil with a 72 mm inner diameter.

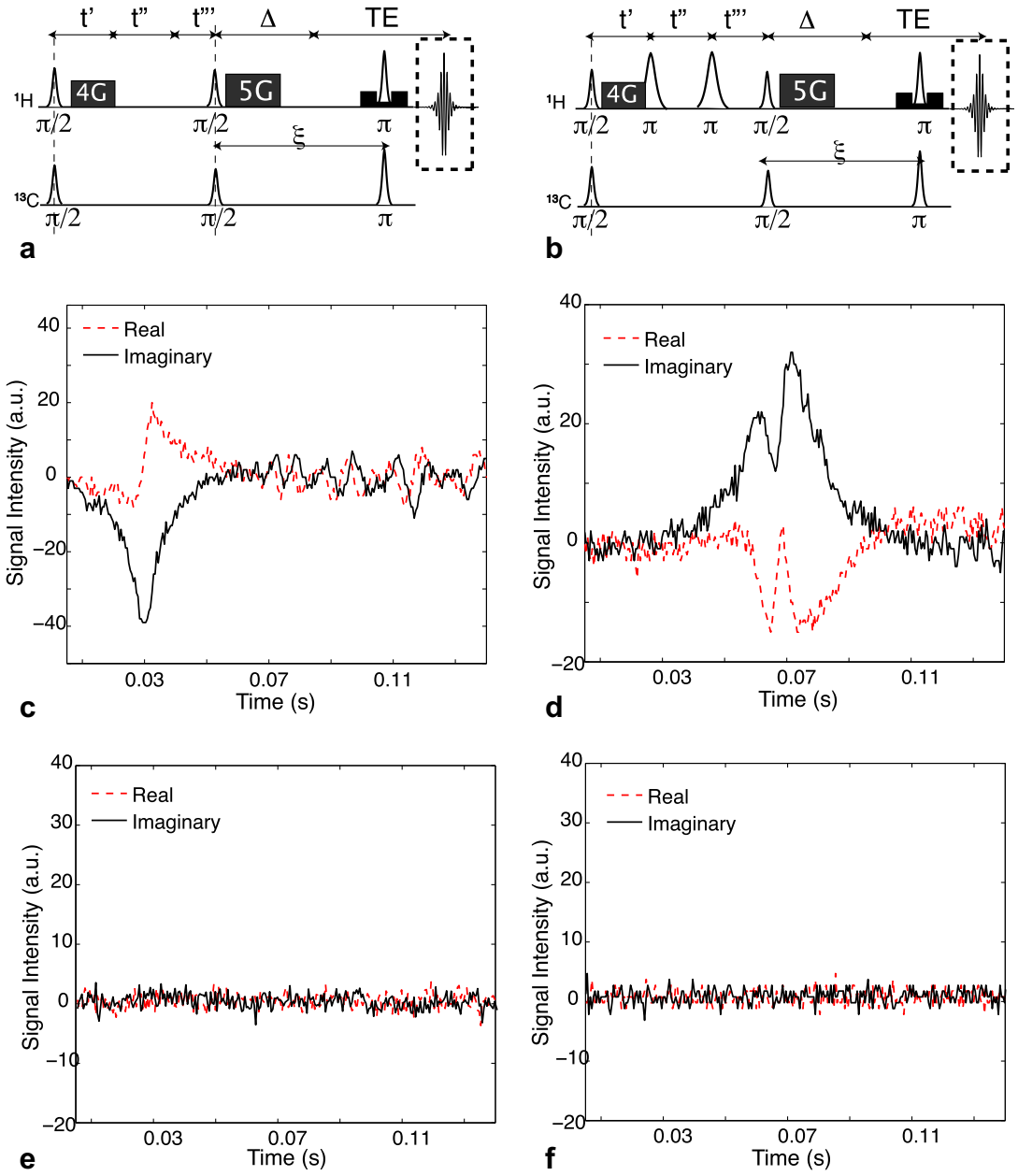

Fig. 3. Comparison between the signal acquired with the ^{13}C–^1H iDQC sequence and the signal acquired with the modified sequence for the pyruvate sample under DNP-enhanced and normal thermal polarization conditions. The ^{13}C–^1H iDQC sequence (a) and the modified sequence (b) have the same iMQC evolution time $t_1 = t' + t'' + t'''$ and the same delay ξ between the mixing pulse and the 180 refocusing pulse. Unlike in (a), the sequence in (b) presents two extra inversion pulses on the ^1H that are used to transform iDQCs into iZQCs and vice versa. (c) Signal acquired with the sequence in figure (a) which refocuses at $\xi-\Delta=\xi-\frac{5}{4}(t'+t''+t''')=30$ ms after the last refocusing pulse. (d) Signal acquired with the sequence in figure (b) which refocuses at $\xi-\Delta=\xi-(\frac{5}{4}(t'+t''')-\frac{3}{4}t'')=70$ ms after the last refocusing pulse. A difference in the refocusing time of 40 ms is noticeable. (e and f) are analogous to (c and d), but recorded after the sample's magnetization has returned to equilibrium.

A 2D spectrum is then acquired from a sample of 1 M ^{13}C enriched urea dissolved in water. This spectrum is acquired with the sequence in Fig. 1b, with a number of averages NA = 80, a repetition time (TR) of 15 s and a spectral bandwidth along the directly detected dimension F2 of SW_{F2} = 1602 Hz. The first excitation pulse and the mixing pulse is set on both ^{13}C and ^{1}H channels to a 90° Hermite pulses, with a duration of 900 μs, while a 1.9 ms Hermite pulse is used to refocus both ^{13}C and ^{1}H spins during the t_2 delay. A 3.5 ms hyperbolic secant pulse is used only on the ^{1}H channel to invert ^{1}H spins during the t_1 delay. The t_1', t_1'', t_1''' and ξ delays are set to 10.25, 17, 1.15 and 60 ms, respectively. The t_1' and t_1'' delays are then incremented 64 times (NR = 64) such that $\Delta t_1' = 937.5\ \mu s$, $\Delta t_1'' = 1562.5\ \mu s$, according to Eq. (4), leading to an indirect spectral bandwidth of $SW_{F1} = \frac{1}{\Delta t_1} = \frac{1}{\Delta t_1' + \Delta t_1''} = \frac{1}{2500\ \mu s} = 400$ Hz. The water resonance frequency offset is then set at +400 Hz, while the carbon offset is set at +200 Hz.

We also acquire a ^{13}C–^{1}H iZQC spectrum on the same sample with the sequence in Fig. 1a, with $G_2/G_1 = -3/4$, t_1 = 28.4 ms and $\Delta t_1 = 2500\ \mu s$. All other parameters are the same as for the previous experiment except for the resonance frequency offset, which in this case is set at 400 Hz for the proton and at 300 Hz for the carbon. In both experiments, the magnetic field is intentionally deshimmed to produce a linewidth of about 200 Hz on the ^{1}H spectrum and 50 Hz on the ^{13}C spectrum (Fig. 2c).

The spectrum acquired with the modified sequence is shown in Fig. 2a, while the spectrum acquired with the ^{13}C–^{1}H iZQC sequence is shown in Fig. 2d. As expected, the ^{13}C–^{1}H correlation appears at $(F1, F2) = (\Omega_C - \frac{\Omega_H}{4}, \Omega_H)_{\substack{\Omega_C = 200\ Hz \\ \Omega_H = 400\ Hz,}} = (100\ Hz, 400\ Hz)$ as expected from Eq. (2), while for the iZQC sequence the peak appears at $(F1, F2) = (\Omega_C - \Omega_H, \Omega_H)_{\substack{\Omega_C = 300\ Hz \\ \Omega_H = 400\ Hz.}} = (-100\ Hz, 400\ Hz)$. A clear line narrowing can be observed between the indirectly detected spectrum of the modified sequence (Fig. 2b) and the standard 1D ^{13}C spectrum (Fig. 2f) and the ^{13}C–^{1}H CRAZED iZQC spectrum (Fig. 2e). While the ^{13}C–^{1}H iZQC resonance frequency line is much broader than the standard 1D ^{13}C resonance frequency line (~75 Hz), the ^{13}C–^{1}H line for the modified sequence appears much narrower than both (~ 20 Hz). In this case the spreading of the ^{13}C resonance frequency is somewhat reduced by subtracting a "renormalized" spreading of the nearby proton spins.

Of course, when high resolution two-dimensional spectroscopy is possible, there are other methods to use iMQCs to effectively remove the inhomogeneous broadening, such as the IDEAL sequence [9]. While 2-D spectroscopy with hyperpolarization has been demonstrated [18], the technique generally relies on uniform resonance frequencies within the sample region, and is thus challenging to extend to imaging.

Aside from 2-D spectroscopy, there is real value in cleaning up the homogeneity of points of the hyperpolarized compounds FID where large signals are expected from the scalar coupling, thereby differentiating nominally similar species. In this spirit, we use the same sequence to collect the echo from a 10 mM hyperpolarized pyruvate sample. For this experiment, the sample is hyperpolarized using the Hypersense Hyperpolarizer from Oxford Instruments. The sample, dissolved in 4.5 mL of DI water with 25 mM EDTA, is polarized for 4 h at a microwave frequency of 94.105 GHz. Just after polarization, the sample is inserted in a 7T small animal imager with a Bruker console. In this case, the delays are set at t' = 13 ms, t'' = 20 ms, and t''' = 3 ms, while the time delay ξ between the mixing pulse and the last 180 refocusing pulse is kept constant at 75 ms. The same experiment is run twice, with and without the selective refocusing pulse on the proton spins (Fig. 3a and b). The different time at which these two signals refocused confirms the different coherence pathways traveled by the spins. Unlike in the iDQC CRAZED sequence, where the signal evolves at 5/4 of the ^{1}H resonance frequency, in the modified sequence the signal evolves during t'' at −3/4 of the ^{1}H resonance frequency. This leads to a different refocusing time, which is given by $(5/4 - (-3/4) * t'' = 40$ ms, as observed in our case (Fig. 3c and d). The same experiments are run again 5 min after dissolution, after the spin system has reached thermal equilibrium (Fig. 3e and f). In this case, almost no signal is observed for both sequences, as expected. This is because the loss of the ^{13}C polarization, for this very low concentration solution, leads to a longer dipolar demagnetization time on the order of several seconds [17], which inherently diminishes the observable signal.

3. Conclusions

We have introduced a modified version of the heteronuclear CRAZED sequence that can be used to indirectly detect inhomogeneity-free spectra from low γ nuclei. We have demonstrated this technique in both thermally polarized samples and in hyperpolarized reagents. Although in the case of hyperpolarized reagents, the sequence needs to be modified to allow the acquisition of an entire 2D spectrum in a single shot, as in [19], our results suggest applications to improving specificity in the detection of hyperpolarized reagents at long echo times, in intrinsically inhomogeneous environments, such as those encountered in standard proton imaging.

Acknowledgment

This work was supported by NIH grant EB02122.

References

[1] Y. Lin, Z. Chen, C. Cai, Z. Chen, High-resolution NMR spectra under inhomogeneous fields via intermolecular double-quantum coherences, Spectrochimica Acta Part A: Molecular and Biomolecular Spectroscopy 70 (5) (2008) 1025–1028.
[2] S. Vathyam, S. Lee, W.S. Warren, Homogeneous NMR spectra in inhomogeneous fields, Science 272 (5258) (1996) 92–96.
[3] Y.Y. Lin, S. Ahn, N. Murali, W. Brey, C.R. Bowers, W.S. Warren, High-resolution, >1 GHz NMR in unstable magnetic fields, Physical Review Letters 85 (17) (2000) 3732.
[4] D. Balla, C. Faber, In vivo intermolecular zero-quantum coherence MR spectroscopy in the rat spinal cord at 17.6 T: a feasibility study, Magnetic Resonance Materials in Physics, Biology and Medicine 20 (4) (2007) 183–191.
[5] W.S. Warren, S. Ahn, M. Mescher, M. Garwood, K. Ugurbil, W. Richter, R.R. Rizi, J. Hopkins, J.S. Leigh, MR imaging contrast enhancement based on intermolecular zero quantum coherences, Science 281 (5374) (1998) 247–251.
[6] R.T. Branca, Y.M. Chen, V. Mouraviev, G. Galiana, E.R. Jenista, C. Kumar, C. Leuschner, S.W. Warren, IDQC anisotropy map imaging for tumor tissue characterization in vivo, Magnetic Resonance in Medicine 61 (4) (2009) 937–943.
[7] W.S. Warren, W. Richter, A. Amy Hamilton, B.T.F. Ii, Generation of impossible cross-peaks between bulk water and biomolecules in solution NMR, Science 262 (5142) (1993) 2005–2009.
[8] G. Galiana, R.T. Branca, E.R. Jenista, W.S. Warren, Accurate temperature imaging based on intermolecular coherences in magnetic resonance, Science 322 (5900) (2008) 421–424.
[9] Z. Chen, Z. Chen, J. Zhong, High-resolution NMR spectra in inhomogeneous fields via IDEAL (intermolecular dipolar-interaction enhanced all lines) method, Journal of the American Chemical Society 126 (2) (2003) 446–447.
[10] C. Zhong, C. Shuhui, C. Zhiwei, Z. Jianhui, Fast acquisition of high-resolution NMR spectra in inhomogeneous fields via intermolecular double-quantum coherences, The Journal of Chemical Physics 130 (8) (2009) 084504.
[11] J. Kurhanewicz, R. Bok, S.J. Nelson, D.B. Vigneron, Current and potential applications of clinical 13C MR spectroscopy, Journal of Nuclear Medicine 49 (3) (2008) 341–344.
[12] K. Golman, Rit Zandt, M. Lerche, R. Pehrson, J.H. Ardenkjaer-Larsen, Metabolic imaging by hyperpolarized 13C magnetic resonance imaging for in vivo tumor diagnosis, Cancer Research 66 (22) (2006) 10855–10860.
[13] M.E. Merritt, C. Harrison, C. Storey, F.M. Jeffrey, A.D. Sherry, C.R. Malloy, Hyperpolarized 13C allows a direct measure of flux through a single enzyme-catalyzed step by NMR, Proceedings of the National Academy of Sciences 104 (50) (2007) 19773–19777.
[14] I.J. Day, J.C. Mitchell, M.J. Snowden, A.L. Davis, Co-acquisition of hyperpolarised 13C and 15N NMR spectra, Magnetic Resonance in Chemistry 45 (12) (2007) 1018–1021.

[15] A.P. Chen, M.J. Albers, C.H. Cunningham, S.J. Kohler, Y.-F. Yen, R.E. Hurd, J. Tropp, R. Bok, J.M. Pauly, S.J. Nelson, J. Kurhanewicz, D.B. Vigneron, Hyperpolarized C-13 spectroscopic imaging of the TRAMP mouse at 3T—Initial experience, Magnetic Resonance in Medicine 58 (6) (2007) 1099–1106.
[16] A.P. Chen, J. Tropp, R.E. Hurd, M.V. Criekinge, L.G. Carvajal, D. Xu, J. Kurhanewicz, D.B. Vigneron, In vivo hyperpolarized 13C MR spectroscopic imaging with 1H decoupling, Journal of Magnetic Resonance 197 (1) (2009) 100–106.
[17] E.R. Jenista, R.T. Branca, W.S. Warren, Hyperpolarized carbon–carbon intermolecular multiple quantum coherences, Journal of Magnetic Resonance 196 (1) (2009) 74–77.
[18] P. Giraudeau, Y. Shrot, L. Frydman, Multiple ultrafast, broadband 2D NMR spectra of hyperpolarized natural products, Journal of the American Chemical Society 131 (39) (2009) 13902–13903.
[19] G. Galiana, R.T. Branca, Warren, Ultrafast intermolecular zero quantum spectroscopy, Journal of the American Chemical Society 127 (50) (2005) 17574–17575.